DMD Fast Forward. Published on March 19, 2020 as DOI: 10.1124/dmd.120.090464
This article has not been copyedited and formatted. The final version may differ from this version.

Title page

Species Differences of Bile Acid Redox Metabolism: Tertiary Oxidation of Deoxycholate is Conserved in Preclinical Animals

Qiuhong Lin[1,4,*], Xianwen Tan[1,4,*], Wenxia Wang[1,4], Wushuang Zeng[1,4], Lanlan Gui[1,4], Mingming Su[2], Changxiao Liu[3], Wei Jia[2], Liang Xu[1], Ke Lan[1,4,#]

[1] Key laboratory of Drug Targeting and Drug Delivery System, Ministry of Education, West China School of Pharmacy, Sichuan University, Chengdu, China.
[2] Metabolomics Shared Resource, University of Hawaii Cancer Center, Honolulu, HI, United States.
[3] State Key Laboratory of Drug Delivery Technology and Pharmacokinetics, Tianjin Institute of Pharmaceutical Research, Tianjin, China.
[4] Chengdu Health-Balance Medical Technology Co., Ltd., Chengdu, China.

Downloaded from dmd.aspetjournals.org at ASPET Journals on April 1, 2020

DMD Fast Forward. Published on March 19, 2020 as DOI: 10.1124/dmd.120.090464
This article has not been copyedited and formatted. The final version may differ from this version.

Running Title Page

Species Differences of Bile Acid Redox Metabolism

 # Corresponding authors

Ke Lan, PhD

West China School of Pharmacy, Sichuan University

No.17 People's South Road, Chengdu, 610041

China

Tel: +86 02885503722

E-mail: lanwoco@scu.edu.cn

Number of text pages: 29

Number of tables: 0

Number of figures: 6

Number of references: 56

Words in Abstract: 240

Words in Introduction: 1081

Words in Methods: 1129

Words in Results: 1269

Words in Discussion: 1155

Downloaded from dmd.aspetjournals.org at ASPET Journals on April 1, 2020

DMD Fast Forward. Published on March 19, 2020 as DOI: 10.1124/dmd.120.090464
This article has not been copyedited and formatted. The final version may differ from this version.

Abbreviations

CA, 3α, 7α, 12α-trihydroxy-5β-cholan-24-oic acid

3-dehydroCA, 3-oxo, 7α, 12α-dihydroxy-5β-cholan-24-oic acid

isoCA, 3β, 7α, 12α-trihydroxy-5β-cholan-24-oic acid

7-oxoDCA, 3α, 7-oxo, 12α-dihydroxy-5β-cholan-24-oic acid

UCA, 3α, 7β, 12α-trihydroxy-5β-cholan-24-oic acid

isoUCA, 3β, 7β, 12α-trihydroxy-5β-cholan-24-oic acid

12-epiCA, 3α, 7α, 12β-trihydroxy-5β-cholan-24-oic acid

DCA, 3α, 12α-dihydroxy-5β-cholan-24-oic acid

isoDCA, 3β, 12α-dihydroxy-5β-cholan-24-oic acid

12-oxoLCA, 3α, 12-oxo-hydroxy-5β-cholan-24-oic acid

12-epiDCA, 3α, 12β-dihydroxy-5β-cholan-24-oic acid

3-dehydroDCA, 3-oxo, 12α-hydroxy-5β-cholan-24-oic acid

DCA-1β-ol, 1β, 3α,12α-trihydroxy-5β-cholan-24-oic acid

DCA-5β-ol, 3α, 5β, 12α-trihydroxy-5β-cholan-24-oic acid

DCA-6α-ol, 3α, 6α, 12α-trihydroxy-5β-cholan-24-oic acid

DCA-6β-ol, 3α, 6β, 12α-trihydroxy-5β-cholan-24-oic acid

DCA-4β-ol, 3α, 4β, 12α-trihydroxy-5β-cholan-24-oic acid

DCA-19-ol, 3α, 12α, 19-trihydroxy-5β-cholan-24-oic acid

CDCA, 3α, 7α-dihydroxy-5β-cholan-24-oic acid

7-oxoLCA, 3α, 7-oxo-hydroxy-5β-cholan-24-oic acid

UDCA, 3α, 7β-dihydroxy-5β-cholan-24-oic acid

isoUDCA, 3β, 7β-dihydroxy-5β-cholan-24-oic acid

LCA, 3α-hydroxy-5β-cholan-24-oic acid

isoLCA, 3β-hydroxy-5β-cholan-24-oic acid

MDCA, 3α, 6β-dihydroxy-5β-cholan-24-oic acid

6-oxoLCA, 3α, 6-oxo-hydroxy-5β-cholan-24-oic acid

HDCA, 3α, 6α-dihydroxy-5β-cholan-24-oic acid

αMCA, 3α, 6β, 7α-trihydroxy-5β-cholan-24-oic acid

βMCA, 3α, 6β, 7β-trihydroxy-5β-cholan-24-oic acid

αHCA, 3α, 6α, 7α-trihydroxy-5β-cholan-24-oic acid

βHCA, 3α, 6α, 7β-trihydroxy-5β-cholan-24-oic acid

NA, not applicable

Downloaded from dmd.aspetjournals.org at ASPET Journals on April 1, 2020

DMD Fast Forward. Published on March 19, 2020 as DOI: 10.1124/dmd.120.090464
This article has not been copyedited and formatted. The final version may differ from this version.

ND, not detected

S_{50}, substrate concentration occupying half of the binding sites

V_{max}, maximal velocity

CL_{int}, intrinsic clearance

LC-MS/MS, liquid chromatography with tandem mass spectrometry

Downloaded from dmd.aspetjournals.org at ASPET Journals on April 1, 2020

Abstract

It was recently disclosed that CYP3A is responsible for the tertiary stereoselective oxidations of deoxycholic acid (DCA), which becomes a continuum mechanism of the host-gut microbial co-metabolism of bile acids (BAs) in human. This work aims to investigate the species difference of BA redox metabolism and clarify whether the tertiary metabolism of DCA is a conserved pathway in preclinical animals. With quantitative determination of the total unconjugated BAs in urine and fecal samples of human, dogs, rats and mice, it was confirmed that the tertiary oxidized metabolites of DCA were found in all tested animals while DCA and its oxidized metabolites disappeared in germ-free mice. The *in vitro* metabolism data of DCA and the other unconjugated BAs in liver microsomes of human, monkeys, dogs, rats and mice showed consistencies with the BA profiling data, confirming that the tertiary oxidation of DCA is a conserved pathway. In liver microsomes of all tested animals, however, the oxidation activities toward DCA were far below the murine-specific 6β-oxidation activities toward chenodeoxycholic acid (CDCA), ursodeoxycholic acid (UDCA) and lithocholic acid (LCA), and 7-oxidation activities toward murideoxycholic acid (MDCA) and hyodeoxycholic acid (HDCA) came from the 6-hydroxylation of LCA. These findings provided further explanations for why murine animals have significantly enhanced downstream metabolism of CDCA compared to human. In conclusion, the species differences of BA redox metabolism disclosed in this work will be useful for the inter-species extrapolation of BA biology and toxicology in translational researches.

Keywords

Primary bile acids; secondary bile acids; tertiary bile acids; species difference; deoxycholate.

Downloaded from dmd.aspetjournals.org at ASPET Journals on April 1, 2020

DMD Fast Forward. Published on March 19, 2020 as DOI: 10.1124/dmd.120.090464
This article has not been copyedited and formatted. The final version may differ from this version.

Significance Statement

It's important to understand the species difference of bile acids metabolism when deciphering biological and hepatotoxicology findings from preclinical studies. However, the species difference of tertiary bile acids is poorly understood compared to primary and secondary bile acids. This work confirmed that the tertiary oxidation of deoxycholic acid is conserved among preclinical animals and provided deeper understanding of how and why the downstream metabolism of chenodeoxycholic acid dominates that of cholic acid in murine animals compared to human.

Downloaded from dmd.aspetjournals.org at ASPET Journals on April 1, 2020

DMD Fast Forward. Published on March 19, 2020 as DOI: 10.1124/dmd.120.090464
This article has not been copyedited and formatted. The final version may differ from this version.

Introduction

Bile acids (BAs) are amphipathic steroids produced almost exclusively by the liver from cholesterol. Most BAs are trapped in the bile acid pool by the process of enterohepatic circulation driven by a series of host-gut microbial metabolism and transport mechanisms (Russell, 2003; Halilbasic et al., 2013; Dawson and Karpen, 2015). As shown in **Figure 1**, this co-metabolism involves metabolic pathways from primary to secondary BAs and from secondary to tertiary BAs, in which the nomenclature of BAs in our work follows Hofmann's proposal (Hofmann et al., 1992). During the enterohepatic circulation of BAs, BA-mediated host-gut microbial crosstalk is important for maintaining a healthy gut microbiota (Theriot et al., 2014; Buffie et al., 2015), balanced lipid and carbohydrate metabolism (de Aguiar Vallim et al., 2013; Wahlstrom et al., 2016), insulin sensitivity (Maruyama et al., 2002; Kawamata et al., 2003), and innate immunity (Inagaki et al., 2006; Vavassori et al., 2009). Drug induced disturbance of BA homeostasis may result in cholestasis and induces hepatic and extrahepatic toxicities, known as drug induced liver injury (DILI). Because there are significant species differences along the host-gut microbiota co-metabolism axis of BAs, DILI is often a poorly predicted adverse event during preclinical studies, and sometimes is unaware until later clinical trials (Chen et al., 2014). As such, it's of great importance to seriously take into account the species difference when deciphering biological and toxicological findings from preclinical animal species.

The species difference of primary BA comes firstly from oxidative on the steroid nucleus and secondly from conjugation with glycine, taurine, sulfate and/or glucuronic acid. Cholic acid (CA) and chenodeoxycholic acid (CDCA) are the primary BAs for most mammals (Hofmann et al., 2010). CDCA may be partly 6α-hydroxylated into α-hyocholic acid (αHCA) by CYP3A (Deo and Bandiera, 2008). Due to the presence of the hepatic 6β-hydroxylase, murine animals have additional primary BAs, known as muricholic acids (αMCA and βMCA) (Hsla et al., 1957; Mahowald et al., 1957a). The murine 6β-hydroxylase was recently identified as CYP2C22 in rats and Cyp2c70 in mice, whose homologous enzyme in human, CYP2C9, is a drug-metabolizing enzyme without BA oxidation activities (Takahashi et al., 2016). Ursodeoxycholic acid (UDCA) is also a primary BA of mice (Sayin et al., 2013) since mice Cyp2c70 is also able to transform CDCA into UDCA (Takahashi et al., 2016). The BAs in humans, minipigs, and hamsters conjugate mainly with glycine, while taurine amidation is predominant in mice, rat and dogs. It has been also discovered that less sulfation occurs in rat and mice compared to human and chimpanzee (Thakare et al., 2018b; Thakare et al., 2018a).

Downloaded from dmd.aspetjournals.org at ASPET Journals on April 1, 2020

DMD Fast Forward. Published on March 19, 2020 as DOI: 10.1124/dmd.120.090464
This article has not been copyedited and formatted. The final version may differ from this version.

The reactions of secondary BAs metabolism greatly enlarge the structural diversity. The major pathway for secondary BAs metabolism is the deconjugation of the amidated primary BAs by bacteria with bile salt hydrolase (BSH) activity (Huijghebaert and Hofmann, 1986; Gopal-Srivastava and Hylemon, 1988) and the subsequent 7-dehydroxylation of the unconjugated forms by bacteria that carry bile acid inducible (Bai) genes (Stellwag and Hylemon, 1979; Hirano et al., 1981; Batta et al., 1990). CA and CDCA are 7-dehydroxylated into deoxycholic acid (DCA) and lithocholic acid (LCA), respectively. UDCA is dehydroxylated into LCA at a similar fashion. The murine-specific BAs, αMCA and βMCA, are 7-dehydroxylated into murideoxycholic acid (MDCA) (Zhang et al., 2012). Another type of reactions of secondary BAs metabolism is epimerization of hydroxyl groups catalyzed by hydroxysteroid dehydrogenases (HSDHs) (Macdonald et al., 1976; MacDonald et al., 1977). CDCA and CA are epimerized into UDCA and ursocholic acid (UCA) and subsequently into isoursodeoxycholic acid (isoUDCA) and isoursocholic acid (isoUCA), respectively (Zhu et al., 2018). CA and DCA are epimerized into 12-epicholic acid (12-epicCA) and 12-epideoxycholic acid (12-epicDCA), respectively (Zhu et al., 2018). To the best of our knowledge, evidences are not yet available for 6-HSDH that may catalyze epimerization between βMCA and β-hyocholic acid (βHCA, also termed ωMCA in literatures) in murine animals (Ridlon et al., 2006; Ridlon et al., 2016). Some of the secondary BAs can be reabsorbed into the liver, where they undergo N-acylamidation metabolism.

Tertiary BAs are redox metabolites of the reabsorbed secondary BAs catalyzed by host enzymes. The term of “tertiary BA” was proposed for the first time based on the identified 7β-oxidation pathway from hyodeoxycholic acid (HDCA) to βHCA after oral administration of HDCA to germ-free rats (Madsen et al., 1975). As a matter of fact, earlier studies have provided evidences for the tertiary BA metabolism by administrating the radiolabeled secondary BAs to bile fistula rats. CDCA, MDCA, αMCA and βMCA were identified as metabolites of LCA (Thomas et al., 1964), MDCA and βHCA were identified as metabolites of HDCA (Matschiner et al., 1957; Matschiner et al., 1958), βMCA was identified as a major metabolite of MDCA (Thomas et al., 1965), CA and DCA-6β-ol were identified as metabolites of DCA (Mahowald et al., 1957b; Ratliff et al., 1961). The murine-specific 7α-hydroxylase, which catalyzes the conversion of DCA and LCA to CA and CDCA in taurine-conjugated forms, respectively, was recently identified as Cyp2a12 in mice (Honda et al., 2020). However, it is much more challenging to study tertiary BA metabolism in larger animals, particularly in human, due to lack of germ-free models and ethnic problems of radiolabeled interventions. Although several BAs with unusual oxidation sites have been

Downloaded from dmd.aspetjournals.org at ASPET Journals on April 1, 2020

DMD Fast Forward. Published on March 19, 2020 as DOI: 10.1124/dmd.120.090464
This article has not been copyedited and formatted. The final version may differ from this version.

identified in humans in the last century (Sjövall et al., 2010), only two CYP3A-catalyzed pathways, 6α-hydroxylation of LCA to HDCA (Trulzsch et al., 1974; Araya and Wikvall, 1999; Deo and Bandiera, 2009) and 1β-hydroxylation of DCA to DCA-1β-ol (Gustafsson et al., 1985; Bodin et al., 2005; Hayes et al., 2016), have been confirmed. The species difference of tertiary BAs is still poorly understood compared to primary and secondary BAs.

We have recently extended the scope of tertiary BA metabolism in human based on BA metabolome analysis in combination with *in vitro* metabolism assays. As shown in **Figure 1**, a series of tertiary oxidation reactions of DCA, glycodeoxycholic acid (GDCA) and taurodeoxycholic acid (TDCA) regioselectively at C-3β, C-1β, C-5β, C-6α, C19, C-4β and C-6β were characterized to be exclusively catalyzed by CYP3A4 and CYP3A7 (Zhang et al., 2019). The 19-hydroxylation of DCA, GDCA and TDCA was identified as a novel *in vitro* marker of CYP3A7 activity (Chen et al., 2019). Following this observation, we confirmed in this work that the tertiary metabolism of DCA is a conserved pathway in commonly used preclinical animal models. A series of murine-specific metabolic pathways that may be responsible for the predominance of downstream metabolism of CDCA in murine animals compared to human were identified and illustrated in **Figure 1**.

Materials and Methods

Materials and Reagents

Authentic standards of 25 unconjugated BAs and 4 stable isotope-labeled internal standards were obtained from Steraloids (Newport, RI), TRC (Toronto, Canada), Santa Cruz (Dallas, TX, USA) or Sigma-Aldrich (St. Louis, MO) as previously described (Zhu et al., 2018). Six DCA metabolites, DCA-1β-ol, DCA-4β-ol, DCA-5β-ol, DCA-6β-ol, DCA-6α-ol and DCA-19-ol, were synthesized as described in our recent report (Zhang et al., 2019). Sulfatase from Helix pomatia Type H-1, β-glucuronidase from Helix pomatia Type H-1 and choloylglycine hydrolase from clostridium perfringens were purchased from Sigma-Aldrich. Human liver microsomes from 150 (76 female and 74 male) mixed gender pooled donors, dogs liver microsomes from 7 (3 female and 4 male) mixed gender pooled donors, rats liver microsomes from 181(21 female and 160 male) mixed gender pooled donors, mice liver microsomes from 170 (150 female and 20 male) mixed gender pooled donors, NADPH regenerating system solution A (NADPH-A, containing 26 mM NADP+, 66 mM glucose-6-phosphate and 66 mM $MgCl_2$ in water), NADPH regenerating system solution B (NADPH-B, containing 40 U/mL glucose-6-phosphate dehydrogenase in 5 mM sodium citrate) and 0.5 M pH 7.4 PBS were purchased from Corning (Tewksbury, MA, USA). Cynomolgus monkeys

Downloaded from dmd.aspetjournals.org at ASPET Journals on April 1, 2020

DMD Fast Forward. Published on March 19, 2020 as DOI: 10.1124/dmd.120.090464
This article has not been copyedited and formatted. The final version may differ from this version.

liver microsomes from 10 (7 female and 3 male) mixed gender pooled donors were purchased from Research Institute for Liver Diseases (Shanghai, China). Sodium acetate, glacial acetic acid, ammonium hydroxide, and LC-MS grade methanol, acetonitrile and formic acid were purchased from Sigma-Aldrich. DMSO was purchased from Thermo Fisher Scientific (Waltham, MA, USA). Ultra-pure water was obtained by using a Milli-Q system (Bedford, MA, USA).

Fecal and Urine Samples

Human fecal and urine samples were collected from healthy volunteers (n=6, 5 female and 1 male) in our laboratory who have signed informed consents. Fecal and urine samples of Beagle dogs (n=6, 3 male and 3 female), Sprague-Dawley rats (n=6, 3 male and 3 female) and C57BL/6 mice (n=8, 4 male and 4 female) were gifted from West China-Frontier PharmaTech (Chengdu, China). Fecal and urine samples of Germ-free C57BL/6 mice (n=3, male) were gifted from Shanghai SLAC Laboratory Animal Co., Ltd (Shanghai, China). The collected samples were stored at -80 °C until analysis.

Sample Preparation for BA Profile Analysis

Quantitative analysis of BA profile was performed using the enzyme digestion techniques (Zhu et al., 2018). In brief, urine and fecal samples were thawed on ice bath. All urine samples were centrifuged at 4°C at 12,000 g for 5 min and 100 μL supernatants from the same species were mixed into a pooled urine sample. Each 50 mg fecal sample was homogenized with 500 μL 0.1% (v/v) ammonium hydroxide solution. The homogenized samples were frozen at - 40°C for 10 min for protein precipitation. The processed samples were centrifuged at 4°C at 12,000 g for 20 min, and 100 μL supernatants from the same species were mixed into a pooled fecal sample. An aliquot (50 μL) of the pooled urine or fecal samples was transferred to 700 μL round well 96-well plate in triplicate. A volume of 150 uL sodium acetate buffer (pH 5.0) containing 50 U of sulfatase, 500 U of β-glucuronidase and 100 U of choloylglycine hydrolase was added to digest the conjugated BAs. The plate was incubated at 37°C for 6 h and subsequently lyophilized. Then, 200 uL of acetonitrile containing 1% formic acid and 100 nM internal standards (LCA-2,2,4,4-D4, DCA-2,2,4,4-D4, UDCA-2,2,4,4-D4 and CA-2,2,4,4-D4) was added in each well. The plate was mixed by vortexing at 1,500 rpm for 30 min at 10°C and then centrifuged at 3,000 g for 20 min at 4°C. The 200 μL supernatant were transferred to another plate and vacuum-evaporated at 30°C. The residue was reconstituted with 50 μL of acetonitrile and 50 μL of

Downloaded from dmd.aspetjournals.org at ASPET Journals on April 1, 2020

DMD Fast Forward. Published on March 19, 2020 as DOI: 10.1124/dmd.120.090464
This article has not been copyedited and formatted. The final version may differ from this version.

water and then mixed by vortexing at 900 rpm for 20 min at 10°C. After centrifugation, the plate was placed into an autosampler for analysis.

In Vitro Oxidation Metabolism Assay

In vitro metabolism was performed using the protocol described in our recent report (Chen et al., 2019; Zhang et al., 2019). In brief, stock solutions of unconjugated BAs were prepared in DMSO. Incubations with an initial substrate concentration of 1.0, 5.0, 25, 50, 100, 200, 300, 500, 750, 1000, 3000, and 5000 μM for DCA were performed in 96-well plates in a shaking incubator at 37°C. Incubations for the other unconjugated BAs were performed with an initial substrate concentration of 50 μM. The 100 μL incubation solution contained 0.1 M PBS (pH 7.4), 5.0 μL NADPH-A, 1.0 μL NADPH-B, 0.5 μL DCA working solution, 0.5 μL blank solvent, and 2.5 μL liver microsomes (protein concentration of 20 mg/mL). The final protein concentration in the incubation media was 0.5 mg/mL. All incubations were performed in triplicate and the DMSO concentration in all incubations was 1% (v/v). The reactions were initiated after 5 min preincubation at 37°C by adding liver microsomes and stopped at a pre-set time point by adding 300 μL of ice-cold acetonitrile containing 0.1% formic acid and 50 μM CA-2,2,4,4-D4 as an internal standard. The reaction mixture was then centrifuged at 4°C at 4000 g for 20 minutes. The supernatant (50 μL) was diluted with 50 μL water and subjected to LC-MS/MS analysis.

Quantitative LC-MS/MS Analysis

Quantitative analysis of unconjugated BAs was performed on ACQUITY ultra-performance liquid chromatography coupled to a Xevo TQ-S mass spectrometer (Waters, Milford, MA, USA) (Yin et al., 2017; Zhu et al., 2018). The mobile phases consisted of 0.01% formic acid in water (mobile phase A) and acetonitrile (mobile phase B). The 5 μL of each sample was injected onto an ACQUITY BEH C18 column (1.7 μm, 100 mm × 2.1 mm) (Waters, Milford, MA). The flow rate was 0.45 mL/min with the following mobile phase gradient: 0.0-0.5 min (95% A), 0.5-1.0 min (95-64% A), 1.0-2.0 min (64-74% A), 2.0-4.0 min (74-70% A), 4.0-6.0 min (70% A), 6.0-7.0 min (70-62% A), 7.0-9.0 min (62-55% A), 9.0-12.5 min (55-30% A), 12.5-13.0 min (30-0% A), 13.0-14.0 min (0% A), 14.0-14.1 (0-95% A) and 14.1-15.0 min (95% A). The mass spectrometer was operated in the negative mode with a 3.0 kV capillary voltage. Selected ion recording for quantification and identification of unconjugated BAs was described in our previous reports (Yin et al., 2017; Zhu et al., 2018; Zhang et al., 2019). The source and desolvation temperatures were set at 150 and 550 °C, respectively. The collision energy was set at 27 V. Nitrogen and argon were used as cone and

Downloaded from dmd.aspetjournals.org at ASPET Journals on April 1, 2020

DMD Fast Forward. Published on March 19, 2020 as DOI: 10.1124/dmd.120.090464
This article has not been copyedited and formatted. The final version may differ from this version.

collision gases, respectively. The cone gas flow and desolvation gas flow were set at 150 and 950 L/h, respectively.

Data processing

The LC-MS/MS raw data was processed by UNIFI (V1.8, Waters, Milford, MA, USA). The metabolite formations as a function of substrate concentrations were fit to Hill (sigmoidal) equation and hyperbolic (Michaelis-Menten) equation using GraphPad Prism software (version 7.0, GraphPad Software, LaJolla, CA).

Results

Tertiary oxidations of deoxycholate is a conserved pathway among the tested animals

In this work, we utilized a pooled-sample strategy to attenuate the intra-species difference and highlight the inter-species difference of the BA profile. Serum or plasma samples were not included in this study due to the known limited exposure of BAs in circulation. A total of 31 unconjugated BAs was quantitated in the pooled urine and fecal samples collected from human, dogs, rats, SPF mice and germ-free mice. These BA metabolites were classified into secondary or tertiary metabolites for the downstream of CA or CDCA (**Figure 2**), based on the known host-gut microbial co-metabolism network of BAs. It was clear that BAs are excreted mainly via feces and minorly via urine. The phenomenon was more significantly observed in murine animals than in human and dogs. The primary BAs, CA and CDCA, and the corresponding secondary BAs, DCA and LCA, respectively, were prevalent in mice, rats, dogs and human. αMCA and βMCA, the 6β-hydroxylated metabolites of CDCA and UDCA, were almost exclusively detected in murine animals, except that αMCA was detected to a much lesser extent in dogs. βMCA, the 6-hydroxyl epimer of βMCA, was exclusively detected in rats and mice. αHCA, a CYP3A-catalyzed 6α-oxidized metabolite of CDCA (Deo and Bandiera, 2008), was detected in human and mice. Comparison between SPF and germ-free mice confirmed that CA, CDCA, UDCA, αMCA and βMCA are the primary BAs of mice, while the other BAs detected in mice are more or less associated with the modification of primary BAs by the host, the secondary metabolism of primary BAs by the gut microbes and/or the tertiary metabolism of reabsorbed secondary BAs by the host.

We have recently characterized both *in vitro* and *in vivo* the tertiary oxidations of DCA, GDCA and TDCA regioselectively at C-1β, C-3β, C-4β, C-5β, C-6α, C-6β and C-19, in which the 3β-hydroxylated metabolite rapidly dehydrates into 3-dehydroDCA (Zhang et al., 2019). This finding was also confirmed in this study that 3-dehydroDCA, DCA-5β-ol, DCA-

Downloaded from dmd.aspetjournals.org at ASPET Journals on April 1, 2020

DMD Fast Forward. Published on March 19, 2020 as DOI: 10.1124/dmd.120.090464
This article has not been copyedited and formatted. The final version may differ from this version.

6α-ol, DCA-4β-ol and DCA-6β-ol were also detected in the feces of dogs, rats and mice (**Figure 2**). DCA-1β-ol was detected in dogs but not in rats and mice. Similar as our recent BA profiling data of human urine, DCA-19-ol, the human CYP3A7-specific tertiary BA metabolite characterized *in vitro*, was not detected in human feces and absent in dogs, rats and mice. Comparison between SPF and germ-free mice showed that both DCA and its downstream tertiary metabolites were absent in germ-free mice. The same pattern was also observed for both LCA and its downstream tertiary metabolites, HDCA and MDCA. Our data has provided a preliminary *in vivo* evidence that the tertiary metabolism of LCA and DCA can be catalyzed by host enzymes.

In vitro metabolite screening of DCA and the other unconjugated monohydroxy or dihydroxy BAs were performed in liver microsomes of dogs, rats, mice, monkeys and human to confirm whether these tertiary BAs found in animals were metabolites uniquely from DCA. Similar to our recent observations in human liver microsomes (Zhang et al., 2019), these tertiary BAs were identified to be neither the di-oxidized metabolites of LCA nor the mono-oxidized metabolites of the other unconjugated dihydroxy BAs (data not shown). As shown in **Figure 3**, a total of 8 oxidized metabolites were continuously produced within 0-720 min after an incubation of 50 μM DCA in liver microsomes of the test species. The DCA oxidations at C-3β, C-1β, C-5β, C-6α, C-4β and C-6β were detected in all the test species, whereas the human CYP3A7-specific metabolite, DCA-19-ol, was not found at a substrate level of 50 μM in the test species. Moreover, rats preferred 7β-oxidation from DCA to UCA, which was commonly considered as the epimerized metabolite of CA mediated by gut microbes. In brief, these results have made it clear that the tertiary oxidation of DCA is a conserved pathway in human, monkeys, dogs, rats and mice.

Species difference of the regioselective oxidation activities of DCA in liver microsomes

Figure 4 showed the apparent kinetic plots of DCA oxidation activities in the liver microsomes of human, monkeys, dogs, rats and mice. Consistent with previous results observed from the recombinant human CYP3A enzymes, oxidation activities gradually reduced to zero for all the species when the concentration of substrates were above 300 μM. The activity loss was probably caused by the protein denaturation of enzymes and/or the formation of multimer and micelle of DCA molecules (Chen et al., 2019). The Hill equation (Supplemental **Table S1**) provides a better fit than the hyperbolic equation (Supplemental **Table S2**) for most kinetic plots within the concentration range from 1 to 300 μM for DCA. The R^2 coefficient for most fittings was >0.99, but lower than that for the none or less productive reactions.

Downloaded from dmd.aspetjournals.org at ASPET Journals on April 1, 2020

Figure 5 illustrated the V_{max}, S_{50} and CL_{int} data obtained from the best curve fitting. Data were calculated predominately using the Hill equation, except that the results for 6β-oxidation in dogs, 3β-oxidation in mice, and 4β-oxidation in mice were calculated using the hyperbolic equation because the Hill-fitting was not applicable. The fitting threshold (300 μM) and critical micelle concentration (CMC, about 1500 μM) of DCA in the incubation media were marked on the S_{50} plot, indicating that all reactions may not achieve the maximum productivity due to the activity loss at substrate levels higher than 300 μM. Anyway, the *in vitro* CL_{int} data represented the intrinsic hepatic metabolic clearance toward DCA under physiological levels. As shown in **Figure 5**, the total clearance of DCA decreased in turn in the liver microsomes of human, monkeys, rats, mice, dogs. In the liver microsomes of the test animals, C-3β, C-1β and C-7β are the major oxidation sites of DCA, while oxidations at the other sites have minor or minimum contribution to the total clearance. A trace activity toward the 19-oxidation of DCA, a human CYP3A7-specific reaction, was detected only in monkeys. The 7β-oxidation of DCA was a rat-specific reaction, which explained well why UCA was found with the highest level in the rat fecal sample. Murine animals showed none or only a trace activity toward the 1β-oxidation of DCA compared to human, monkeys and dogs, which was consistent with that DCA-1β-ol was not detected in rats and mice.

In vitro reactions responsible for the murine-specific downstream metabolism of CDCA

It was recently discovered that rat CYP2C22 and mouse Cyp2c70 are responsible for the murine-specific 6β-oxidation from CDCA to αMCA and UDCA to βMCA (Takahashi et al., 2016). Cyp2a12 was recently reported to be responsible for the 7α-oxidation from TDCA to TCA and TLCA to TCDCA (Honda et al., 2020). Thus, the species difference of BA metabolism between murine and the others observed in our study may also indicate that CDCA metabolism appears to be superior to CA metabolism in murine animals. We therefore investigated the oxidation metabolism of the downstream metabolites of CDCA, including CDCA, UDCA, LCA, HDCA and MDCA (50 μM), in liver microsomes of murine animals in contrast to the other species. In this way, a series of murine-specific metabolic reactions were identified. As shown in **Figure 6**, these reactions revealed not only the known 6β-oxidation from CDCA to αMCA and UDCA to βMCA, but also the 6β-oxidation from LCA to MDCA, the 7α-oxidation from MDCA to αMCA, and the rat-specific 7β-oxidation from MDCA to βMCA and HDCA to βHCA. Theses murine-specific oxidation activities were much higher than their activities toward DCA oxidations (**Figure 2**). The 7α-oxidation from DCA to CA and LCA to CDCA was not detected, which is consistent with that conjugated BAs are much better substrates for Cyp2a12 than unconjugated BAs in mice (Honda et al., 2020).

Downloaded from dmd.aspetjournals.org at ASPET Journals on April 1, 2020

DMD Fast Forward. Published on March 19, 2020 as DOI: 10.1124/dmd.120.090464
This article has not been copyedited and formatted. The final version may differ from this version.

Discussion

By using BA profiling technique in combination with the *in vitro* metabolism assays, this work has confirmed that tertiary oxidation of DCA is a conserved pathway in human, monkeys, dogs, rats and mice. The BA profiling data between SPF mice and germ-free mice has provided preliminary *in vivo* evidence that the host liver is responsible for the tertiary metabolism of DCA. Future works addressing dispositions of oral DCA in germ-free mice may provide direct evidences to identify how the host eliminates DCA without colonization of gut microbiota. Species differences in the oxidation regioselectivity of DCA were shown by the apparent oxidation kinetics of DCA in the pooled liver microsomes of animals. Most of the *in vitro* kinetic data was consistent with the BA profiling data, in which all conjugated forms (N-amidated forms, sulfated forms and glucuronidated forms) were detected as unconjugated forms by using the enzyme-digestion techniques in the present work. Some *in vitro* - *in vivo* data inconsistency may be associated with the N-acylamidation metabolism of BAs, which has been shown to have an impact on the activity and regioselectivity of DCA oxidation in human (Zhang et al., 2019). Deeper understanding of the species difference relies on development of the next-generation BA profiling techniques including not only N-amidated forms but also sulfated forms and glucuronidated forms of BAs.

Our previous work has demonstrated that renal clearance of the tertiary metabolites of DCA is significantly higher than that of DCA and CA, indicating that tertiary BA metabolism facilitates, at least in part, the renal excretion of DCA (Zhang et al., 2019). Similarly, 12-epiDCA, a epimerized microbial metabolite of DCA, was also inclined to be excreted in urine, where it was detected mainly as amidated forms (Zhu et al., 2018). In this work, a total of 9 downstream metabolites of DCA was detected in human urine and feces, including 3 microbial metabolites (isoDCA, 12-epiDCA and 12-oxoLCA) and 6 tertiary metabolites (3-dehydroDCA, DCA-6β-ol, DCA-5β-ol, DCA-6α-ol, DCA-1β-ol, and DCA-4β-ol). Two microbial metabolites of DCA, 12-epiDCA and 12-oxoLCA, were detected in both urine and feces, while isoDCA was only found in feces. Consistent with our previous data, all these tertiary metabolites of DCA were detected in urine except for 3-dehydroDCA, which was detected with much higher level in feces than the other tertiary metabolites. Nevertheless, the microbial metabolites of DCA had higher levels than the tertiary metabolites in urine and particularly feces. Therefore, DCA appeared to be disposed mainly by microbial metabolism and fecal excretion and complementally by hepatic tertiary metabolism and renal excretion in human. As illustrated in **Figure 2**, the disposition pathways of DCA are relatively conserved

Downloaded from dmd.aspetjournals.org at ASPET Journals on April 1, 2020

DMD Fast Forward. Published on March 19, 2020 as DOI: 10.1124/dmd.120.090464
This article has not been copyedited and formatted. The final version may differ from this version.

in the tested animals, which might have explained why a slight decrease of TDCA was observed without significance in the liver and gallbladder of Cyp3a knock out (KO) mice compared to the wild-type littermate controls (Wahlstrom et al., 2017).

This work also has provided deeper understanding of how and why the species difference of BA metabolism between murine and the other animals occurs more in the downstream metabolism of CDCA than that of CA. As shown in **Figure 2**, CA metabolism prevails over CDCA metabolism in human and dogs while CDCA metabolism is significantly enhanced in murine animals, particularly in rats. The underlying mechanism is clearly shown by that the murine animals have strong 6β-hydroxylation activities toward the downstream metabolites of CDCA. In liver microsomes of all tested animals, the oxidation activities toward DCA (**Figure 3**) are far below the murine-specific oxidation activities toward CDCA, UDCA and LCA (**Figure 6**). Therefore, the 6β-oxidation of CDCA and UDCA constitute the major pathway to synthesis of αMCA and βMCA. Moreover, murine animals also have a specific tertiary pathway for the 6β-oxidation from LCA to MDCA, and the 7α- and 7β-oxidation from MDCA to αMCA and βMCA, which furnish an alternative pathway to synthesis αMCA and βMCA. In these ways, CDCA, UDCA and LCA in murine animals are almost completely transformed into the more polar 6β-hydroxylated BAs, αMCA, βMCA and MDCA. In contrast, due to the lack of 6β-oxidation activities, human and dogs have evolved the BA metabolism patterns dominated by the downstream metabolism of CA and DCA.

However, the host-responsible *in vitro* reactions carried out in this work did not well explain the murine-specific synthesis of βHCA. Although rats liver microsomes were able to oxidize HDCA at C-7β into βHCA, both rats and mice had limited activities toward the 6α-oxidation from LCA to HDCA. A recent study also found no significant differences of βHCA and TβHCA in Cyp3a KO mice compared to the wild-type controls (Wahlstrom et al., 2017). Therefore, we deduced that tertiary metabolism of LCA contribute less to the production of HDCA and βHCA compared to the microbial modifications of αMCA and βMCA (Eyssen et al., 1999). Our deduction was consistent with that from a recent study of BA metabolism in Cyp2a12 KO, Cyp2c70 KO, and Cyp2a12/Cyp2c70 double KO mice (Honda et al., 2020). Future studies are required to characterize the microbial 6-HSDHs that are potentially responsible for the 6-epimerization reactions between βMCA and βHCA in murine animals.

In conclusion, this work demonstrated that the tertiary oxidation of DCA is a conserved BA metabolism pathway in preclinical animals. The orthologous genes of human CYP3A are believed to be responsible for the tertiary oxidation of DCA in animals. In the tested animals, the majority of DCA synthesized by microbes in lower gut is disposed by microbial

Downloaded from dmd.aspetjournals.org at ASPET Journals on April 1, 2020

DMD Fast Forward. Published on March 19, 2020 as DOI: 10.1124/dmd.120.090464
This article has not been copyedited and formatted. The final version may differ from this version.

metabolism and undergoes fecal excretion, while the tertiary metabolism of DCA might have physiologically constituted a complementary disposition mechanism of DCA. The conclusion was consistent with that Cyp3a KO did not significantly alter the major BA composition in mice (Wahlstrom et al., 2017). Compared to human and dogs, murine animals favored the downstream metabolism of CDCA, mainly due to the presence of the strong hepatic 6β-oxidation activities towards CDCA, UDCA, LCA and 7-oxidation activities towards MDCA and HDCA, the 6-hydroxylated metabolites of LCA. The murine-specific 6β-hydroxylase was identified as CYP2C22 in rats and Cyp2c70 in mice (Takahashi et al., 2016). The mouse-specific 7α-hydroxylase responsible for hydroxylating TDCA into TCA and TLCA into TCDCA was identified as Cyp2a12 (Honda et al., 2020). These P450s are believed to produce a murine-specific hydrophilic BA composition, which partly explains why murine animals are relatively resistant to hepatobiliary toxicities caused by accumulation of hydrophobic BAs. Cyp2c70 KO, Cyp2a12 KO, and Cyp2c70/Cyp2a12 double KO mice have been characterized to produce more human-like hydrophobic BA composition (de Boer et al., 2019; Honda et al., 2020). Although the tertiary BAs were not studied in these works, the expression and activity of Cyp3a11 was found to be complementarily induced in Cyp2c70/Cyp2a12 double KO mice via activation of pregnane X receptor and/or constitutive androstane receptor. Collectively based on these evidences, the genetic modified murine animal models that knock out murine-specific BA metabolizing P450 genes are believed to be promising interspecies scaling tools for future studies of BA associated signaling, metabolism, drug metabolism and toxicology.

Acknowledgments

We are grateful to Mr. Bing Liu and Ms. Lian Yang (West China-Frontier PharmaTech) for the gift of animal urine and fecal samples.

Authorship Contributions

Participated in research design: Lan.
Conducted experiments: Lin, Tan, Wang, Zeng, Gui, Su, Lan.
Contributed metabolite synthesis: Xu.
Performed data analysis: Lan, Lin, Tan.
Wrote or contributed to the writing of the manuscript: Lan, Su, Jia, Liu, Lin, Tan.

References

Downloaded from dmd.aspetjournals.org at ASPET Journals on April 1, 2020

DMD Fast Forward. Published on March 19, 2020 as DOI: 10.1124/dmd.120.090464
This article has not been copyedited and formatted. The final version may differ from this version.

Araya Z and Wikvall K (1999) 6α-Hydroxylation of taurochenodeoxycholic acid and lithocholic acid by CYP3A4 in human liver microsomes. *Biochim Biophys Acta* **1438:**47-54.

Batta AK, Salen G, Arora R, Shefer S, Batta M, and Person A (1990) Side chain conjugation prevents bacterial 7-dehydroxylation of bile acids. *J Biol Chem* **265:**10925-10928.

Bergström S, Danielsson H, and Göransson A (1959) On the bile acid metabolism in the pig. Bile acids and steroids 81. *Acta Chem Scand* **13:**776-783.

Bodin K, Lindbom U, and Diczfalusy U (2005) Novel pathways of bile acid metabolism involving CYP3A4. *Biochim Biophys Acta* **1687:**84-93.

Buffie CG, Bucci V, Stein RR, McKenney PT, Ling L, Gobourne A, No D, Liu H, Kinnebrew M, Viale A, Littmann E, van den Brink MR, Jenq RR, Taur Y, Sander C, Cross JR, Toussaint NC, Xavier JB, and Pamer EG (2015) Precision microbiome reconstitution restores bile acid mediated resistance to Clostridium difficile. *Nature* **517:**205-208.

Chen M, Borlak J, and Tong W (2014) Predicting idiosyncratic drug-induced liver injury: some recent advances. *Expert Rev Gastroenterol Hepatol* **8:**721-723.

Chen YJ, Zhang J, Zhu PP, Tan XW, Lin QH, Wang WX, Yin SS, Gao LZ, Su MM, Liu CX, Xu L, Jia W, Sevrioukova IF, and Lan K (2019) Stereoselective Oxidation Kinetics of Deoxycholate in Recombinant and Microsomal CYP3A Enzymes: Deoxycholate 19-Hydroxylation Is an In Vitro Marker of CYP3A7 Activity. *Drug Metab Dispos* **47:**574-581.

Dawson PA and Karpen SJ (2015) Intestinal transport and metabolism of bile acids. *J Lipid Res* **56:**1085-1099.

de Aguiar Vallim TQ, Tarling EJ, and Edwards PA (2013) Pleiotropic roles of bile acids in metabolism. *Cell Metab* **17:**657-669.

de Boer JF, Verkade E, Mulder NL, de Vries HD, Huijkman NCA, Koehorst M, Boer T, Wolters JC, Bloks VW, van de Sluis B, and Kuipers F (2019) A Human-like Bile Acid Pool Induced by Deletion of Cyp2c70 Modulates Effects of Farnesoid X Receptor Activation in Mice. *J Lipid Res*:jlr.RA119000243.

Deo AK and Bandiera SM (2008) Identification of human hepatic cytochrome p450 enzymes involved in the biotransformation of cholic and chenodeoxycholic acid. *Drug Metab Dispos* **36:**1983-1991.

Deo AK and Bandiera SM (2009) 3-ketocholanoic acid is the major in vitro human hepatic microsomal metabolite of lithocholic acid. *Drug Metab Dispos* **37:**1938-1947.

Eyssen HJ, De Pauw G, and Van Eldere J (1999) Formation of hyodeoxycholic acid from muricholic acid and hyocholic acid by an unidentified gram-positive rod termed HDCA-1 isolated from rat intestinal microflora. *Appl Environ Microbiol* **65:**3158-3163.

Gopal-Srivastava R and Hylemon PB (1988) Purification and characterization of bile salt hydrolase from Clostridium perfringens. *J Lipid Res* **29:**1079-1085.

Gustafsson J, Andersson S, and Sjovall J (1985) Bile acid metabolism during development: metabolism of taurodeoxycholic acid in human fetal liver. *Biol Neonate* **47:**26-31.

Halilbasic E, Claudel T, and Trauner M (2013) Bile acid transporters and regulatory nuclear receptors in the liver and beyond. *J Hepatol* **58:**155-168.

Haslewood GA (1954) "Hyocholic acid", a trihydroxy bile acid from pig bile. *Biochem J* **56:**xxxviii.

Hayes MA, Li XQ, Gronberg G, Diczfalusy U, and Andersson TB (2016) CYP3A Specifically Catalyzes 1beta-Hydroxylation of Deoxycholic Acid: Characterization and Enzymatic Synthesis of a Potential Novel Urinary Biomarker for CYP3A Activity. *Drug Metab Dispos* **44:**1480-1489.

Hirano S, Nakama R, Tamaki M, Masuda N, and Oda H (1981) Isolation and characterization of thirteen intestinal microorganisms capable of 7 alpha-dehydroxylating bile acids. *Appl Environ Microbiol* **41:**737-745.

Hofmann AF, Hagey LR, and Krasowski MD (2010) Bile salts of vertebrates: structural variation and possible evolutionary significance. *J Lipid Res* **51:**226-246.

Hofmann AF, Sjovall J, Kurz G, Radominska A, Schteingart CD, Tint GS, Vlahcevic ZR, and Setchell KD (1992) A proposed nomenclature for bile acids. *J Lipid Res* **33:**599-604.

Honda A, Miyazaki T, Iwamoto J, Hirayama T, Morishita Y, Monma T, Ueda H, Mizuno S, Sugiyama F, Takahashi S, and Ikegami T (2020) Regulation of bile acid metabolism in mouse models with hydrophobic bile acid composition. *J Lipid Res* **61:**54-69.

Downloaded from dmd.aspetjournals.org at ASPET Journals on April 1, 2020

DMD Fast Forward. Published on March 19, 2020 as DOI: 10.1124/dmd.120.090464
This article has not been copyedited and formatted. The final version may differ from this version.

Hsla SL, Matschiner JT, Mahowald TA, Elliott WH, Doisy EA, Jr., Thayer SA, and Doisy EA (1957) Bile acids. VI. The structure and synthesis of acid II. *J Biol Chem* **226:**667-671.

Huijghebaert SM and Hofmann AF (1986) Influence of the amino acid moiety on deconjugation of bile acid amidates by cholylglycine hydrolase or human fecal cultures. *J Lipid Res* **27:**742-752.

Inagaki T, Moschetta A, Lee YK, Peng L, Zhao G, Downes M, Yu RT, Shelton JM, Richardson JA, Repa JJ, Mangelsdorf DJ, and Kliewer SA (2006) Regulation of antibacterial defense in the small intestine by the nuclear bile acid receptor. *Proc Natl Acad Sci U S A* **103:**3920-3925.

Kawamata Y, Fujii R, Hosoya M, Harada M, Yoshida H, Miwa M, Fukusumi S, Habata Y, Itoh T, Shintani Y, Hinuma S, Fujisawa Y, and Fujino M (2003) A G protein-coupled receptor responsive to bile acids. *J Biol Chem* **278:**9435-9440.

Lundell K (2004) The porcine taurochenodeoxycholic acid 6alpha-hydroxylase (CYP4A21) gene: evolution by gene duplication and gene conversion. *Biochem J* **378:**1053-1058.

Lundell K, Hansson R, and Wikvall K (2001) Cloning and expression of a pig liver taurochenodeoxycholic acid 6alpha-hydroxylase (CYP4A21): a novel member of the CYP4A subfamily. *J Biol Chem* **276:**9606-9612.

MacDonald IA, Mahony DE, Jellet JF, and Meier CE (1977) NAD-dependent 3alpha- and 12alpha-hydroxysteroid dehydrogenase activities from Eubacterium lentum ATCC no. 25559. *Biochim Biophys Acta* **489:**466-476.

Macdonald IA, Meier EC, Mahony DE, and Costain GA (1976) 3alpha-, 7alpha- and 12alpha-hydroxysteroid dehydrogenase activities from Clostridium perfringens. *Biochim Biophys Acta* **450:**142-153.

Madsen DC, Chang L, and Wostmann B (1975) Omega-muricholate: a tertiary bile acid of the Wistar rat. *Proc Indiana Acad Sci* **84:**416-420.

Mahowald TA, Matschiner JT, Hsia SL, Doisy EA, Jr., Elliott WH, and Doisy EA (1957a) Bile acids. III. Acid I; the principal bile acid in urine of surgically jaundiced rats. *J Biol Chem* **225:**795-802.

Mahowald TA, Matschiner JT, Hsia SL, Richter R, Doisy EA, Jr., Elliott WH, and Doisy EA (1957b) Bile acids. II. Metabolism of deoxycholic acid-24-C14 and chenodeoxycholic acid-24-C14 in the rat. *J Biol Chem* **225:**781-793.

Maruyama T, Miyamoto Y, Nakamura T, Tamai Y, Okada H, Sugiyama E, Nakamura T, Itadani H, and Tanaka K (2002) Identification of membrane-type receptor for bile acids (M-BAR). *Biochem Biophys Res Commun* **298:**714-719.

Matschiner JT, Mahowald TA, Hsia SL, Doisy EA, Jr., Elliott WH, and Doisy EA (1957) Bile acids. IV. The metabolism of hyodeoxycholic acid-24-C14. *J Biol Chem* **225:**803-810.

Matschiner JT, Ratliff RL, Mahowald TA, Doisy EA, Jr., Elliott WH, Hsia SL, and Doisy EA (1958) Bile acids. IX. Metabolites of hyodeoxycholic acid-24-C14 in surgically jaundiced rats. *J Biol Chem* **230:**589-596.

Ratliff RL, Matschiner JT, Doisy EA, Jr., Hsia SL, Thayer SA, Elliott WH, and Doisy EA (1961) Bile acids. XV. Partial synthesis of the new metabolite of deoxycholic acid, 3 alpha,6 beta,12 alpha-trihydroxycholanic acid. *J Biol Chem* **236:**685-687.

Ridlon JM, Harris SC, Bhowmik S, Kang DJ, and Hylemon PB (2016) Consequences of bile salt biotransformations by intestinal bacteria. *Gut Microbes* **7:**22-39.

Ridlon JM, Kang DJ, and Hylemon PB (2006) Bile salt biotransformations by human intestinal bacteria. *J Lipid Res* **47:**241-259.

Russell DW (2003) The enzymes, regulation, and genetics of bile acid synthesis. *Annu Rev Biochem* **72:**137-174.

Sayin SI, Wahlstrom A, Felin J, Jantti S, Marschall HU, Bamberg K, Angelin B, Hyotylainen T, Oresic M, and Backhed F (2013) Gut microbiota regulates bile acid metabolism by reducing the levels of tauro-beta-muricholic acid, a naturally occurring FXR antagonist. *Cell Metab* **17:**225-235.

Sjövall J, Griffiths WJ, Setchell KD, Mano N, and Goto J (2010) Analysis of bile acids in Steroid analysis(Makin HL and Gower D eds) pp 837-966, Springer, Dordrecht.Stellwag EJ and Hylemon PB (1979) 7alpha-Dehydroxylation of cholic acid and chenodeoxycholic acid by Clostridium leptum. *J Lipid Res* **20:**325-333.

Downloaded from dmd.aspetjournals.org at ASPET Journals on April 1, 2020

DMD Fast Forward. Published on March 19, 2020 as DOI: 10.1124/dmd.120.090464
This article has not been copyedited and formatted. The final version may differ from this version.

Takahashi S, Fukami T, Masuo Y, Brocker CN, Xie C, Krausz KW, Wolf CR, Henderson CJ, and Gonzalez FJ (2016) Cyp2c70 is responsible for the species difference in bile acid metabolism between mice and humans. *J Lipid Res* **57:**2130-2137.

Thakare R, Alamoudi JA, Gautam N, Rodrigues AD, and Alnouti Y (2018a) Species differences in bile acids I. Plasma and urine bile acid composition. *J Appl Toxicol : JAT* **38:**1323-1335.

Thakare R, Alamoudi JA, Gautam N, Rodrigues AD, and Alnouti Y (2018b) Species differences in bile acids II. Bile acid metabolism. *J Appl Toxicol : JAT* **38:**1336-1352.

Theriot CM, Koenigsknecht MJ, Carlson PE, Jr., Hatton GE, Nelson AM, Li B, Huffnagle GB, J ZL, and Young VB (2014) Antibiotic-induced shifts in the mouse gut microbiome and metabolome increase susceptibility to Clostridium difficile infection. *Nat Commun* **5:**3114.

Thomas PJ, Hsia SL, Matschiner JT, Doisy EA, Jr., Elliott WH, Thayer SA, and Doisy EA (1964) Bile Acids. Xix. Metabolism of Lithocholic Acid-24-14c in the Rat. *J Biol Chem* **239:**102-105.

Thomas PJ, Hsia SL, Matschiner JT, Thayer SA, Elliott WH, Doisy EA, Jr., and Doisy EA (1965) Bile Acids. Xxi. Metabolism of 3-Alpha,6-Beta-Dihydroxy-5-Beta-Cholanoic Acid-24-C 14-6-Alpha-H3 in the Rat. *J Biol Chem* **240:**1059-1063.

Trulzsch D, Roboz J, Greim H, Czygan P, Rudick J, Hutterer F, Schaffner F, and Popper H (1974) Hydroxylation of taurolithocholate by isolated human liver microsomes. I. Identification of metabolic product. *Biochem Med* **9:**158-166.

Vavassori P, Mencarelli A, Renga B, Distrutti E, and Fiorucci S (2009) The bile acid receptor FXR is a modulator of intestinal innate immunity. *J Immunol* **183:**6251-6261.

Wahlstrom A, Al-Dury S, Stahlman M, Backhed F, and Marschall HU (2017) Cyp3a11 is not essential for the formation of murine bile acids. *Biochemistry and biophysics reports* **10:**70-75.

Wahlstrom A, Sayin SI, Marschall HU, and Backhed F (2016) Intestinal Crosstalk between Bile Acids and Microbiota and Its Impact on Host Metabolism. *Cell Metab* **24:**41-50.

Yin S, Su M, Xie G, Li X, Wei R, Liu C, Lan K, and Jia W (2017) Factors affecting separation and detection of bile acids by liquid chromatography coupled with mass spectrometry in negative mode. *Anal Bioanal Chem* **409:**5533-5545.

Zhang J, Gao LZ, Chen YJ, Zhu PP, Yin SS, Su MM, Ni Y, Miao J, Wu WL, Chen H, Brouwer KLR, Liu CX, Xu L, Jia W, and Lan K (2019) Continuum of Host-Gut Microbial Co-metabolism: Host CYP3A4/3A7 Are Responsible for Tertiary Oxidations of Deoxycholate Species. *Drug Metab Dispos* **47:**283-294.

Zhang Y, Limaye PB, Lehman-McKeeman LD, and Klaassen CD (2012) Dysfunction of organic anion transporting polypeptide 1a1 alters intestinal bacteria and bile acid metabolism in mice. *PLoS One* **7:**e34522.

Zhu P, Zhang J, Chen Y, Yin S, Su M, Xie G, Brouwer KLR, Liu C, Lan K, and Jia W (2018) Analysis of human C24 bile acids metabolome in serum and urine based on enzyme digestion of conjugated bile acids and LC-MS determination of unconjugated bile acids. *Anal Bioanal Chem* **410:**5287-5300.

Downloaded from dmd.aspetjournals.org at ASPET Journals on April 1, 2020

DMD Fast Forward. Published on March 19, 2020 as DOI: 10.1124/dmd.120.090464
This article has not been copyedited and formatted. The final version may differ from this version.

Footnotes

* Q.-H. L. and X.-W. T. contributed equally to this work.

This work was supported partly by the Fundamental Research Funds for the Central Universities and the 111 Project of the National Ministry of Education (B18035).

Downloaded from dmd.aspetjournals.org at ASPET Journals on April 1, 2020

DMD Fast Forward. Published on March 19, 2020 as DOI: 10.1124/dmd.120.090464
This article has not been copyedited and formatted. The final version may differ from this version.

Figure Legends

Figure 1. Metabolic scheme of the primary BAs to secondary BAs to tertiary BAs pathways. The abbreviated nomenclature of unconjugated bile acids follows Hofmann's proposal (Hofmann et al., 1992). The structures of conjugated forms and oxo- or keto- intermediates were not shown.

Figure 2. Quantitative profiles of the total unconjugated BAs in the pooled urine and fecal samples of human (n=6), dogs (n=6), rats (n=6), SPF mice (n=8) and germ-free mice (n=3). The unconjugated BAs were quantitatively determined by treating samples with choloylglycine hydrolase, sulfatase and β-glucuronidase as the method described previously. Data was shown as mean ±SD for triplicate analysis of the pooled samples.

Figure 3. Time-dependent metabolite formation after incubation of DCA (50 μM) in the liver microsomes (protein level 0.5 mg/mL) of human, monkeys, dogs, rats and mice. Data was shown as mean± SD (n=3).

Figure 4. Kinetic plots of DCA oxidations in the liver microsomes (protein level 0.5 mg/mL) of human, monkeys, dogs, rats and mice. The dotted extrapolations of Hill curves demonstrate a violation of enzyme kinetics at higher substrate levels (>300 μM). Data was shown as mean± SD (n=3).

Figure 5. Apparent Hill parameters of DCA oxidation in the liver microsomes (protein level 0.5 mg/mL) of human, monkeys, dogs, rats and mice fitted with Hill equation (1-300 μM).

Figure 6. Metabolite formation after incubation of LCA, CDCA, UDCA, HDCA and MDCA (50 μM) in the liver microsomes (protein level 0.5 mg/mL) of human, monkeys, dogs, rats and mice for 60 min. Data was shown as mean± SD (n=3) in pmol/min/mg protein.

Downloaded from dmd.aspetjournals.org at ASPET Journals on April 1, 2020

DMD Fast Forward. Published on March 19, 2020 as DOI: 10.1124/dmd.120.090464
This article has not been copyedited and formatted. The final version may differ from this version.

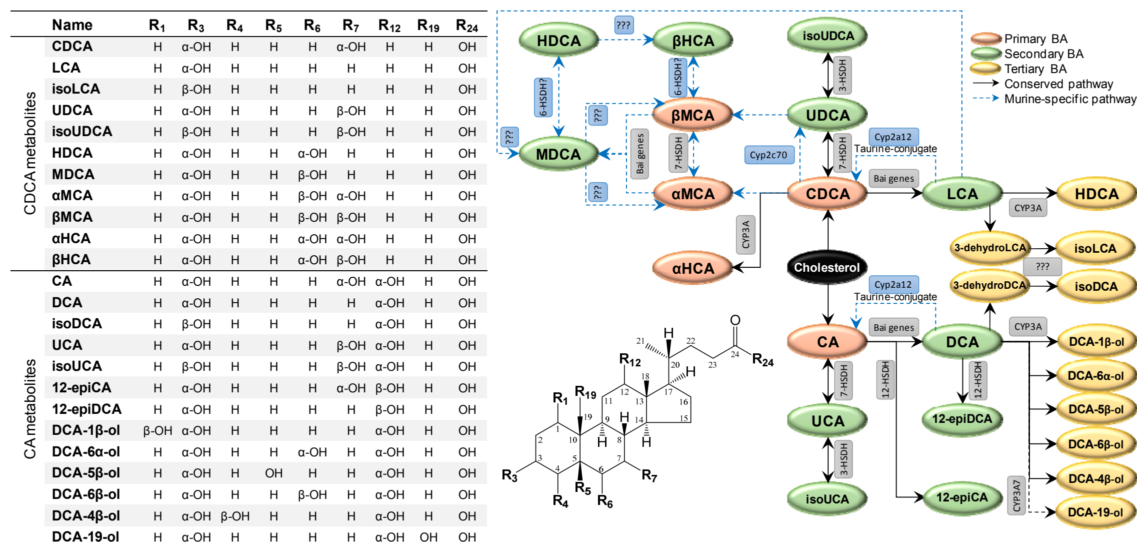

	Name	R_1	R_3	R_4	R_5	R_6	R_7	R_{12}	R_{19}	R_{24}
CDCA metabolites	**CDCA**	H	α-OH	H	H	H	α-OH	H	H	OH
	LCA	H	α-OH	H	H	H	H	H	H	OH
	isoLCA	H	β-OH	H	H	H	H	H	H	OH
	UDCA	H	α-OH	H	H	H	β-OH	H	H	OH
	isoUDCA	H	β-OH	H	H	H	β-OH	H	H	OH
	HDCA	H	α-OH	H	H	α-OH	H	H	H	OH
	MDCA	H	α-OH	H	H	β-OH	H	H	H	OH
	αMCA	H	α-OH	H	H	β-OH	α-OH	H	H	OH
	βMCA	H	α-OH	H	H	β-OH	β-OH	H	H	OH
	αHCA	H	α-OH	H	H	α-OH	α-OH	H	H	OH
	βHCA	H	α-OH	H	H	α-OH	β-OH	H	H	OH
CA metabolites	**CA**	H	α-OH	H	H	H	α-OH	α-OH	H	OH
	DCA	H	α-OH	H	H	H	H	α-OH	H	OH
	isoDCA	H	β-OH	H	H	H	H	α-OH	H	OH
	UCA	H	α-OH	H	H	H	β-OH	α-OH	H	OH
	isoUCA	H	β-OH	H	H	H	β-OH	α-OH	H	OH
	12-epiCA	H	α-OH	H	H	H	α-OH	β-OH	H	OH
	12-epiDCA	H	α-OH	H	H	H	H	β-OH	H	OH
	DCA-1β-ol	β-OH	α-OH	H	H	H	H	α-OH	H	OH
	DCA-6α-ol	H	α-OH	H	H	α-OH	H	α-OH	H	OH
	DCA-5β-ol	H	α-OH	H	OH	H	H	α-OH	H	OH
	DCA-6β-ol	H	α-OH	H	H	β-OH	H	α-OH	H	OH
	DCA-4β-ol	H	α-OH	β-OH	H	H	H	α-OH	H	OH
	DCA-19-ol	H	α-OH	H	H	H	H	α-OH	OH	OH

Figure 1

Downloaded from dmd.aspetjournals.org at ASPET Journals on April 1, 2020

DMD Fast Forward. Published on March 19, 2020 as DOI: 10.1124/dmd.120.090464
This article has not been copyedited and formatted. The final version may differ from this version.

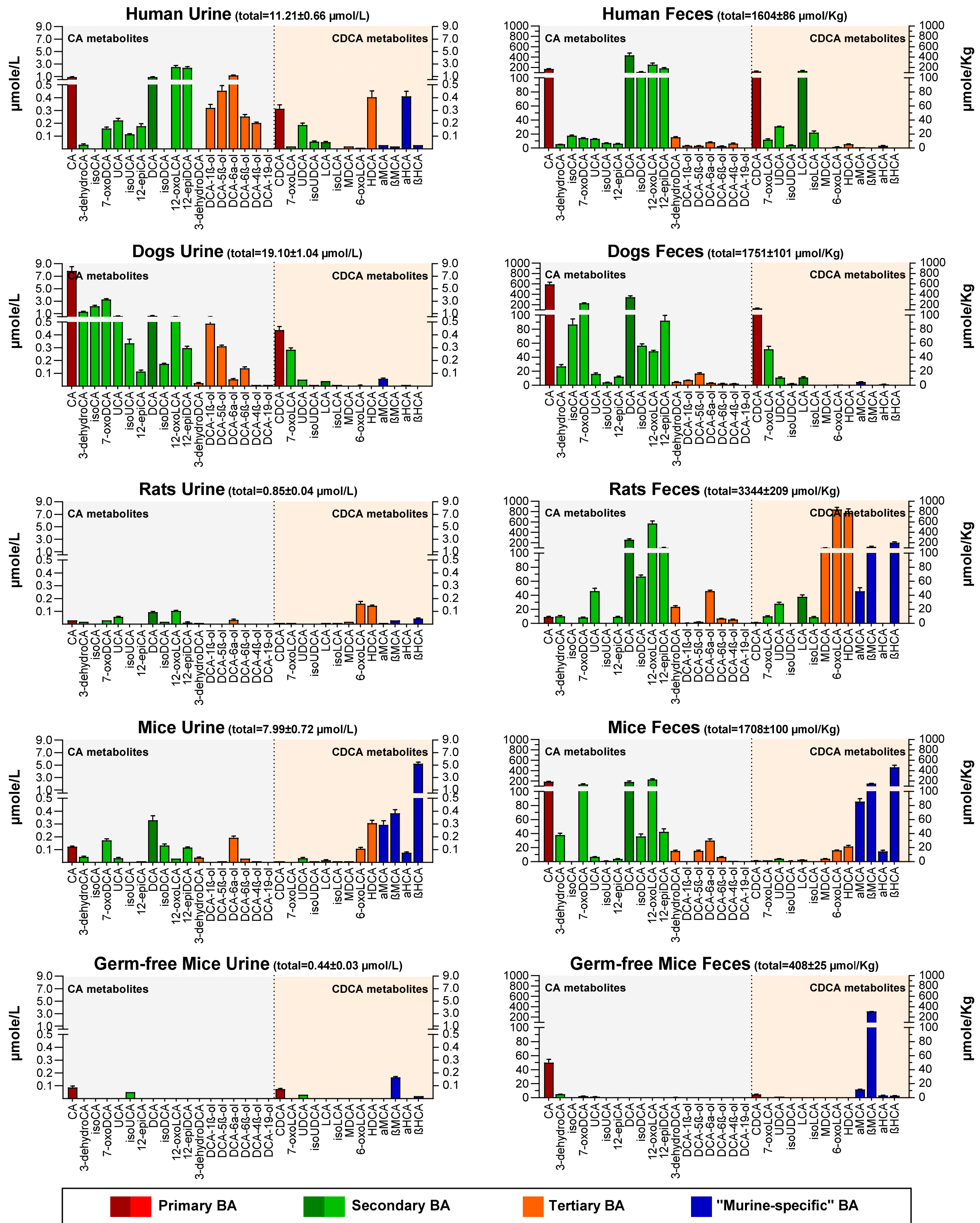

Figure 2

Downloaded from dmd.aspetjournals.org at ASPET Journals on April 1, 2020

DMD Fast Forward. Published on March 19, 2020 as DOI: 10.1124/dmd.120.090464
This article has not been copyedited and formatted. The final version may differ from this version.

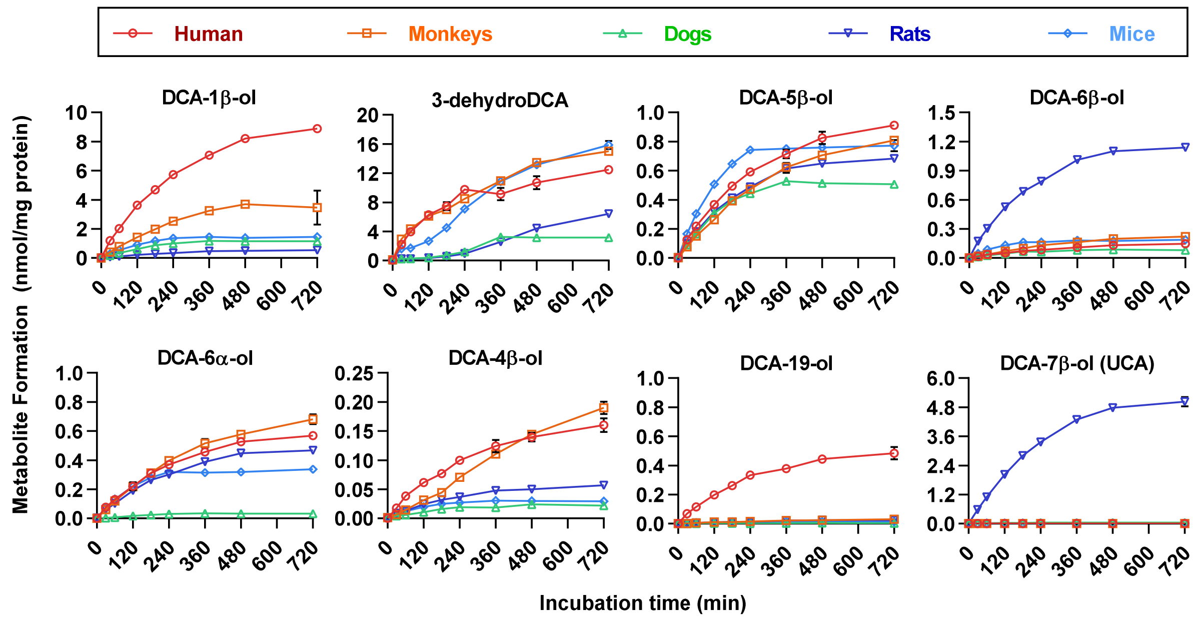

Figure 3

Downloaded from dmd.aspetjournals.org at ASPET Journals on April 1, 2020

DMD Fast Forward. Published on March 19, 2020 as DOI: 10.1124/dmd.120.090464
This article has not been copyedited and formatted. The final version may differ from this version.

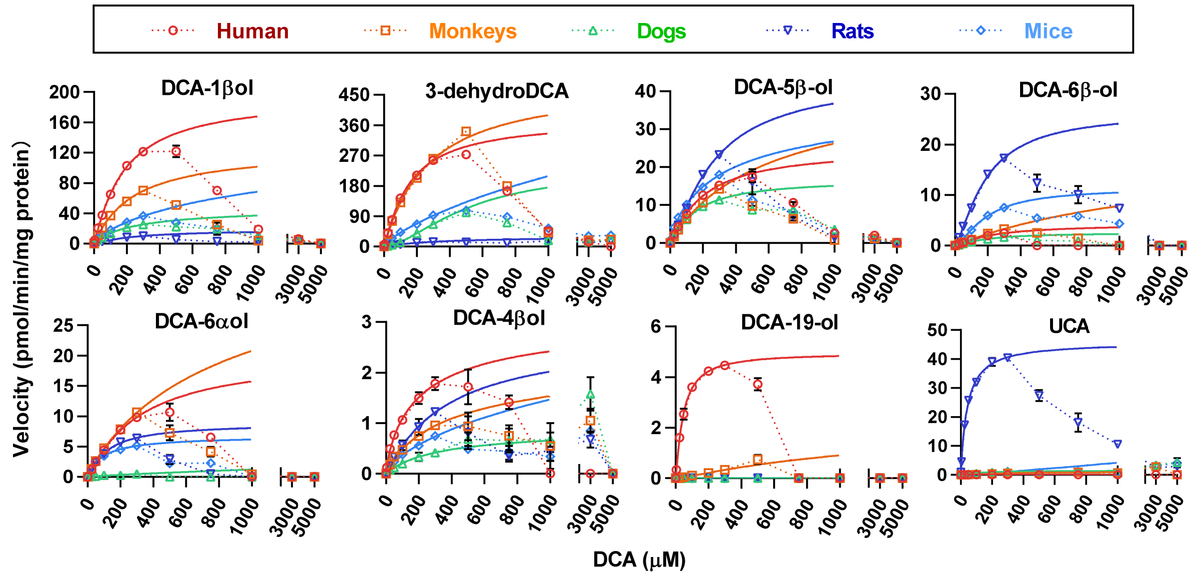

Figure 4

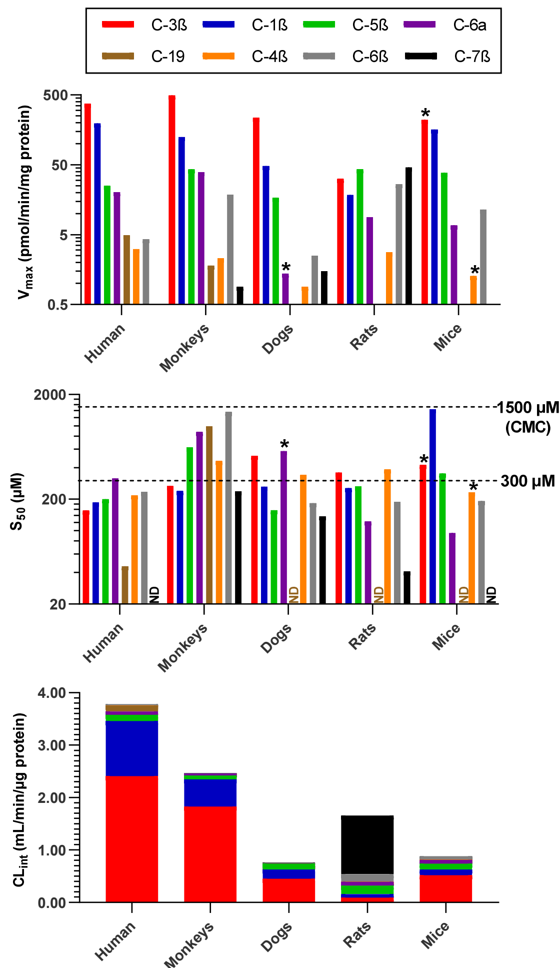

Figure 5

Downloaded from dmd.aspetjournals.org at ASPET Journals on April 1, 2020

DMD Fast Forward. Published on March 19, 2020 as DOI: 10.1124/dmd.120.090464
This article has not been copyedited and formatted. The final version may differ from this version.

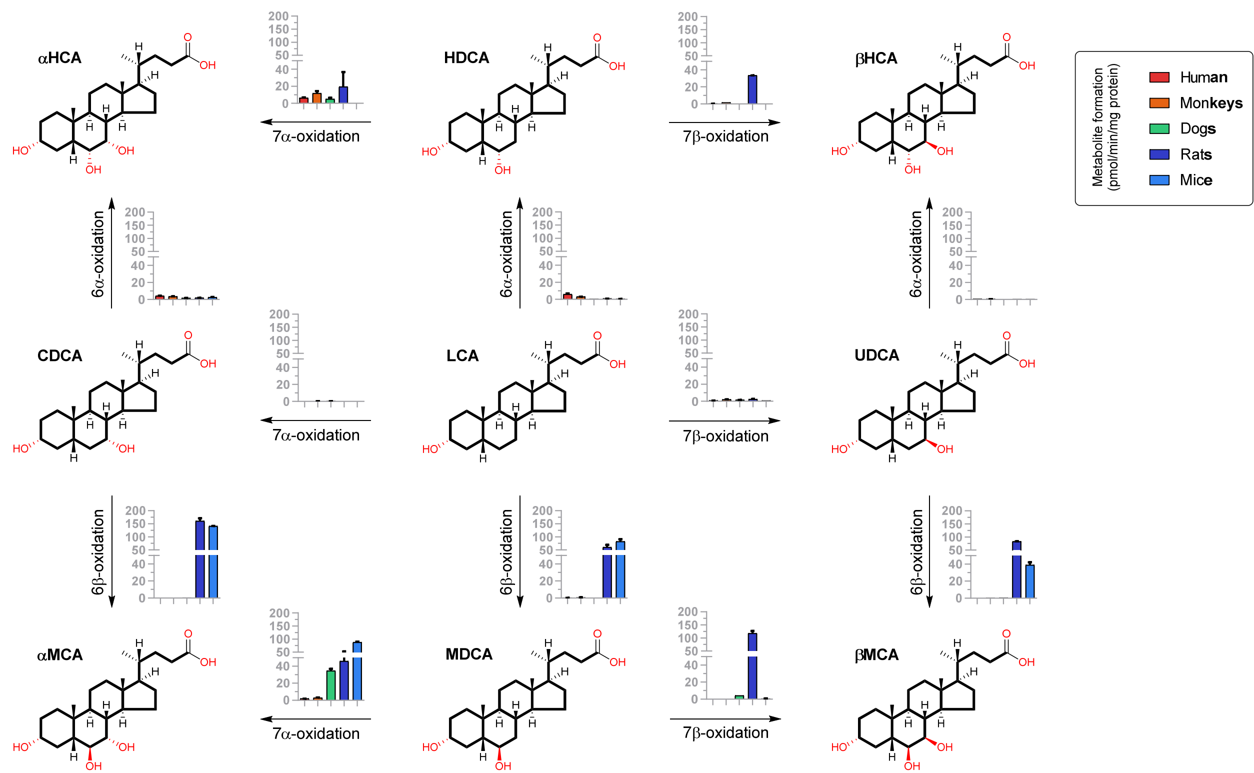

Figure 6

Downloaded from dmd.aspetjournals.org at ASPET Journals on April 1, 2020